J Exp Biol Advance Online Articles. First posted online on 19 July 2017 as doi:10.1242/jeb.156695
Access the most recent version at http://jeb.biologists.org/lookup/doi/10.1242/jeb.156695

Physiological responses to fluctuating temperatures are characterized by distinct transcriptional profiles in a solitary bee

Alex S. Torson*[1], George D. Yocum[2], Joseph P. Rinehart[2],
Sean A. Nash[1], Kally M. Kvidera[1], Julia H. Bowsher[1]

[1]North Dakota State University, Department of Biological Sciences, P.O. Box 6050, Fargo ND 58108 USA

[2]USDA-ARS Red River Valley Agricultural Research Center, Biosciences Research Laboratory, 1605 Albrecht Boulevard, Fargo, ND 58102-2765 USA

* Corresponding author: Alex S. Torson: Alex.S.Torson@ndsu.edu

Key words: FTR, *Megachile rotundata*, temperature stress, fluctuating thermal regime

Summary Statement

Transcriptional responses to fluctuating thermal regimes differ between life stages in the alfalfa leafcutting bee, *Megachile rotundata.*

Abstract

Exposure to stressful low temperatures during development can result in the accumulation of deleterious physiological effects called chill injury. Metabolic imbalances, disruptions in ion homeostasis, and oxidative stress contribute to the increased mortality of chill-injured insects. Interestingly, survival can be significantly increased when chill susceptible insects are exposed to a daily warm-temperature pulse during chilling. We hypothesize that warm pulses allow for the repair of damage associated with chill-injury. Here, we describe transcriptional responses during exposure to a fluctuating thermal regime (FTR), relative to constant chilled temperatures, during pupal development in the alfalfa leafcutting bee, *Megachile rotundata* using a combination of RNA-seq and qPCR. Pupae were exposed to either a constant, chilled temperature of 6°C, or 6°C with a daily pulse of 20°C for seven days. RNA-seq after experimental treatment revealed differential expression of transcripts involved in construction of cell membranes, oxidation-reduction and various metabolic processes. These mechanisms provide support for shared physiological responses to chill injury across taxa. The large number of differentially expressed transcripts observed after seven days of treatment suggests that the initial divergence in expression profiles between the two treatments occurred upstream of the time point sampled. Additionally, the differential expression profiles observed in this study show little overlap with those differentially expressed during temperature stress in the diapause state of *M. rotundata*. While the mechanisms governing the physiological response to low-temperature stress are shared, the specific transcripts associated with the response differ between life stages.

Introduction

In ectothermic animals like insects, environmental temperatures play a critical role in the animal's physiology. Exposure to stressful, low temperatures during development can have significant, detrimental effects on adult insects (Bale and Hayward, 2010; Bennett et al., 2013; O'Neill et al., 2011; Whitfield and Richards, 1992; Yocum et al., 1994; Yocum et al., 2006). The degree to which insects respond to these temperature stressors is highly dependent upon the timing, duration, and amplitude of exposure (Colinet et al., 2015). With global climate change threatening to increase temperature variance (Easterling et al., 2000; Hansen et al., 2012), insects will likely be faced with increased exposure to low, seasonally unpredictable temperatures (Vasseur et al., 2014). In chill-susceptible insects, prolonged exposure to low temperatures can lead to the accumulation of deleterious physiological effects called chill injury (Lee, 2010).

Chill injury causes significant increases in mortality (Colinet et al., 2011; Kostál, 2006; Lee, 2010; Renault et al., 2004). The downstream physiological consequences of chill injury are complex but appear to be caused in part by membrane phase transitions (Lee, 2010). Damage to cell membranes results in metabolic imbalances and perturbations in ion homeostasis (Kostál, 2004; Kostál et al., 2006) that have been observed in chill-injured insects. Furthermore, temperature stress is associated with oxidative stress (Lalouette et al., 2011; Rojas and Leopold, 1996) and impairment of neuromuscular system function (Bennett et al., 2015; Yocum et al., 1994); both of which are implicated as downstream consequences of cell membrane damage (Lee, 2010).

The decreased survival and cellular damage associated with chill injury can be mitigated by exposure to transient, daily increases in temperature during chilling (termed fluctuating thermal regimes; FTR). Exposure to these brief, daily temperature increases during chilling results in increases in survival in chill-injured insects (Chen and Denlinger, 1992; Colinet et al., 2006; Colinet et al., 2007; Jing et al., 2005; Kostál et al., 2007; Kostál et al., 2016; Leopold et al., 1998; Marshall and Sinclair, 2012; Renault et al., 2004; Rinehart et al., 2011; Yocum et al., 2012). Exposure to FTR during chilling allows for either the protection against or repair of damage caused by chill injury (Colinet et al., 2015; Lee, 2010). While it is possible that brief, daily exposure to warmer temperatures during chilling allows for a physiological preparation (i.e. protection) for chilling, the hypothesis that exposure to warmer temperatures allows reparative mechanisms to act has more empirical support (Colinet et al., 2006; Kostál et al., 2007; Nedvěd et al., 1998; Torson et al., 2015). FTR repairs chill injury damage in many taxa (Boardman et al., 2013; Jing et al., 2005; Kostál et

al., 2007; Leopold et al., 1998; Nedvěd et al., 1998; Renault et al., 2004), but it is unclear whether the mechanisms governing the beneficial effects associated with FTR exposure are conserved.

Current management practices for the solitary bee, *Megachile rotundata*, a valuable agricultural pollinator, can include stressful low temperature exposure at two life stages: prepupal post-diapause quiescence and pupal development. *M. rotundata* females emerge and provision offspring in the early summer. Larvae complete growth in about a week and enter a prepupal diapause for overwintering. Under commercial management, the overwintering period lasts 7-10 months (Pitts-Singer and Crane 2011), but can be artificially extended to over a year (Rinehart et al. 2013). However, extended overwintering causes chill injury (Rinehart et al. 2013; Torson et al. 2015). In the spring, managers increased storage temperatures to initiate pupation and adult eclosion. If weather delays peak floral bloom, managers slow pupal development using low temperatures. Low temperature exposure during pupation also leads to chill injury (Rinehart et al. 2011). Diapausing prepupae and developing pupae are very different life stages both physiologically and molecularly (MacRae, 2010). Interestingly, exposure to FTR during low temperature exposure increases survival in both contexts (Rinehart et al. 2011, Rinehart et al. 2013), and reduces the sub-lethal effects of chill injury (Bennett et al., 2015).

Gene expression comparisons could reveal whether the response to FTR is conserved across different developmental stages of *Megachile rotundata*. An RNA-seq study conducted in post-diapause quiescent prepupal *M. rotundata* provided support for the physiological evidence in other chill-injured insects and offered insight into mechanisms driving the reparative effect of FTR versus exposure to a constant 6°C (Torson et al., 2015). Individuals exposed to FTR had increased expression of transcripts functioning in the maintenance of ion homeostasis, response to oxidative stress, and an increase in metabolic function; all congruent with the hypothesis that FTR allows for repair of damage during the warm phase. These transcriptional profiles could represent a conserved mechanism. Given that FTR has similar protective effects on survival in both overwintering prepupae and pupae exposed to cold during development, we hypothesized a conserved suite of genes would underlie the response. The goals of our study were to 1) identify differential gene expression in individuals exposed to FTR protocol during pupal development and 2) determine if expression profiles observed in pupal FTR support a conserved reparative mechanism of FTR across life stages in *M. rotundata*. Developing pupae were exposed to either a constant, low-temperature stress (static thermal regime, STR) or the same low temperature with a daily,

one-hour warm-temperature pulse for seven days (FTR). RNA was harvested from bees exposed to either treatment after the warm pulse on day seven. We hypothesized that, as a result of a conserved mechanism driving the reparative effect of FTR across taxa, the exposure to fluctuating temperatures during low temperature stress during this life stage would elicit transcriptional responses similar to prepupal responses observed previously (Torson et al., 2015).

Materials and Methods

Temperature protocols

M. rotundata were purchased from JWM Leafcutter, Inc. (Nampa, ID), and were of Canadian origin. Diapausing prepupae arrived as loose cells and were housed in Percival model I-30BLL reach-in incubators at 6°C ± 0.5°C under darkness until initiation of the experiment. To end overwinting and initiate development, prepupae were transferred to a Percival model I-30BLL at 29°C. To assess the progression of pupal development prior to treatment, bees not destined for experimental treatment were dissected out of their brood cells and placed them in 24-well plates to function as guide plates. The guide plates were stored in plastic containers with breathable lids and a saturated NaCl solution was used to maintain humidity at 75% (as described in Winston and Bates, 1960). Experimental bees were maintained at 29°C until ~50% of the bees in the guide plates reached a developmental stage characterized by melanization of the eyes, called the “red eye” stage. At the red-eye stage, bees were grouped into one of two treatments: a Fluctuating Thermal Regime (FTR) or Static Thermal Regime (STR; Fig. 1). Bees reared under the FTR protocol were exposed to 6°C with a daily warm pulse of 20°C consisting of a 1 h ramp up to 20°C (0.23°C/ min), a 1 h incubation at 20°C, and a 1 h ramp down, back to 6°C for each of the seven days of treatment. Those reared under the STR treatment were maintained at 6°C for the duration of the seven-day treatment.

Bees used in the experiments were collected over two field seasons. The RNA-seq and validation was conducted on bees derived from the 2013 summer field season, which arrived in the lab in late March 2014. The qPCR time series was conducted on bees derived from the 2014 summer field season, which arrived in the lab in late March 2015. Before arriving at the lab, prepupal were overwintered at a constant temperature (4-6°C) by the supplier (JWM Leafcutter, Inc).

RNA-seq

RNA Collection

Total RNA was collected from whole *M. rotundata* pupae exposed to either the FTR or STR treatment (3 biological replicates per treatment; 1 biological replicate is one individual). To ensure the assessment of response to low temperature exposure and not a warm-temperature exposure, individuals from both treatments were harvested for RNA during the cold phase (6°C; Fig. 1) and maintained on ice until the animals were sacrificed. Animals were harvested during the cold phase (after FTR warm pulse) to ensure a measurement of low temperature response in both treatments. Samples were harvested shortly after (~1hr) the warm pulse in the event that the effect was transient. Pupae were transferred directly from ice and homogenized in 500 µl of TRIzol using a polypropylene pestle in a nuclease free 1.5 ml microcentrifuge tube. The Invitrogen TRIzol protocol (Carlsbad, CA USA) was followed for RNA extraction. Final product was stored as an ethanol precipitate at -80°C until needed.

RNA-seq Library Preparation and Sequencing

Prior to sequencing, RNA pellets were dissolved in DEPC-treated H_2O and shipped at a concentration of no less than 20 ng/ul (~10ug total RNA) on dry ice overnight to the University of Georgia. Upon arrival to the University of Georgia Genomics Facility (Athens, GA USA), RNA samples from both FTR and STR treatments were checked for quality using an Aligent Bioanalyzer (Santa Clara, CA USA). A total of 4µg of total RNA was used for input in the Illumina Truseq Stranded mRNA kit. Samples were pooled and run on a NextSeq500 using a Version 1 Mid-Output 300 cycle kit with PE150 settings. Demultiplexing and adapter trimming were done by default when data was processed on BaseSpace (Illumina, San Diego, CA USA).

Differential Expression Analysis

Raw sequence data (BioProject Accession: PRJNA352846) were quality checked using FastQC (Version 0.10.1; Babraham Bioinformatics). TopHat (Verse 2.0.9) was used to align the raw reads against the *M. rotundata* reference genome (BioProject Accession: PRJNA66515). Assembly of mapped reads was conducted using Cufflinks (Version 2.0.2) and differential expression analysis was carried out using Cuffdiff (Version 2.0.2) via the iPlant Collaborative Discovery Environment (Stanzione, 2011). Transcripts were considered significantly differentially expressed when the *q-value* (Benjamini-Hochberg-corrected *p-*

value) was below the false discovery rate (FDR) of 0.05. The R package cummeRbund (Trapnell et al., 2012) and the Java-based functional annotation program Blast2GO (Conesa et al. 2005) were used for downstream analysis and the generation of differential expression figures.

Life-stage-specific RNA-seq comparison

To assess whether significant overlap between gene expression profiles exist during low-temperature stress between post-diapause quiescent prepupae (Torson et al., 2015) and developing pupae Venn diagrams were constructed using the R package VennDiagram (Chen and Boutros, 2011). Statistical significance of the overlap of differentially expressed transcripts between data sets was determined via hypergeometric distribution using the R function phyper. The total number of transcripts for comparison was 11,195, which is the total number of transcripts in the reference transcriptome for *M. rotundata*.

RNA-seq Validation:

RNA collection:

Residual RNA from each RNA-seq sample (2013 field season; described above) was aliquoted and stored at -80°C under ethanol and used for the qPCR validation of the computational methods described above. The 10 most upregulated transcripts in response to FTR were selected for validation.

Sample preparation

RNA samples were diluted to a concentration of 0.333 µg/µl and subsequently treated with Invitrogen DNAase I (Carlsbad, CA, USA) to remove genomic DNA contaminants. A total of 1 µg RNA for each of the three biological replicates per treatment was used as template for first strand cDNA synthesis using Invitrogen Super Script III first strand synthesis system for RT-PCR (Carlsbad, CA, USA).

qPCR

Real-time quantitative PCR reactions were conducted on a Roche LightCycler 480 II (Indianapolis, ID, USA) using Roche FastStart Universal SYBR Green I Master Mix with ROX (Indianapolis, IN, USA). Primers for all targets (10 most upregulated transcripts from RNA-seq experiment, Table S1) and eight reference gene candidates were designed using Integrated DNA Technologies IDR program (Coralville, IA, USA). Candidate reference

genes were selected using this RNA-seq data set and libraries generated in Torson et al. 2015 (18 libraries total) to identify stably expressed transcripts. Expression of differentially expressed transcripts in qPCR runs were normalized against two most stably expressed reference targets identified using the algorithm geNorm (Vandesompele et al., 2002).

To ensure quality control between and within plates, three controls were used on each plate: a "no template control" consisting of all enzymatic components without cDNA template, a "negative RT control" lacking reverse transcriptase, and a "positive RT control" using a control cDNA template and control primers for each plate. The "positive RT control" also served as calibrator reactions in the event that comparisons spanned multiple plates.

Biogazelle qbase+ (Ghent, Belgium) and Prism Graphpad (La Jolla, CA USA) were used for statistical analysis and graphical representations of the data respectively. Statistical significance for each of the 10 upregulated and 8 non-differentially expressed transcripts was determined by T-test of the calibrated normalized relative quantity (CNRQ) of each transcript from qbase+.

qPCR Time Series

RNA collection:

M. rotundata from the 2014 field season were reared at 29°C until eye pigmentation stage and then split into either the FTR or STR protocol described above. Total RNA for the qPCR time series was collected from whole *M. rotundata* pupae exposed to either the FTR or STR treatment (6 biological replicates; 1 individual per replicate). Before exposure to treatment, pupae were harvested to serve as a baseline for gene expression (T_0; Fig. 1). After placement into treatment, individuals were sacrificed during the cold phase (6°C, shortly after the warm pulse in FTR) for each of the seven days of treatment (T_1-T_7; Fig. 1). Animals were placed on ice during dissection from brood cells until they were homogenized for RNA extraction to prevent an additional warm-temperature exposure. The Invitrogen TRIzol protocol (Carlsbad, CA USA) was followed for RNA extraction. Final product was stored as an ethanol precipitate at -80°C until needed. Sample preparation, qPCR runs and similarly to RNA-seq validation (see previous section). Two-way ANOVA with Bonferroni's correction for multiple comparisons determined statistical significance of differential expression and relationships across time, within treatments were determined using linear regression.

Results

Assembly:

Three biological replicates were harvested from each treatment, totaling six individual transcriptomic libraries (BioProject Accession: PRJNA352846). Each library averaged a total of 47,279,330 reads (Table 1). Raw reads were mapped to the *M. rotundata* reference genome (BioProject Accession: PRJNA66515) with an average alignment rate of 69.11%. FastQC (Version 0.10.1; Babraham Bioinformatics) was used to determine baseline quality of raw reads and percentage of reads mapped to the reference genome and mate pair concordance (Table 1) were used as a metric of assembly quality.

Differential Expression Analysis and Validation:

Using the Tuxedo protocol (Trapnell et al., 2012), expression analysis revealed a total of 434 differentially expressed transcripts between STR and FTR treatments after seven days of exposure to treatment (307 downregulated and 127 upregulated in FTR). Real-time quantitative PCR confirmed the expression profiles of 8 transcripts upregulated in FTR, relative to STR and 6 non-differentially expressed transcripts that we used as reference gene candidates (Table S2). Differential expression was confirmed in all cases with at least one primer pair. We were able to confirm expression of 8 of the top 10 FTR-upregulated transcripts (Table S2, S3) and 6 of 8 non-differentially-expressed transcripts (Table S3).

Gene Ontology:

A Benjamini and Hochberg corrected Fisher's exact test (one tailed, FDR=0.05) of up- and downregulated transcripts in response to FTR revealed no over or underrepresented functional classes relative to the GO distribution in the reference transcriptome. Due to the lack of enrichment for GO terms, relative to the reference transcriptome, we used direct counts of GO terms of the differentially expressed transcripts in this study for downstream analyses and discussions. Direct counts of the transcripts differentially expressed between FTR and STR treatments on T_7 of treatment revealed classes of transcripts functioning in biological processes including regulation of transcription, oxidation-reduction, signal transduction, and various metabolic processes (Fig. S1). Also, a direct count of biological process GO terms (Fig. 2) revealed the upregulation in FTR of transcripts functioning in signal transduction and trans-membrane transport. Furthermore, GO terms associated with the construction of cellular components, including plasma membrane and various membrane components were upregulated in response to FTR (Fig 2).

Life-stage-specific comparisons:

When the identities of differentially expressed transcripts observed in this study are compared with those presented during the two time points assessed during post-diapause quiescence (Torson et al., 2015), 30 (6.9%) differentially expressed transcripts in the pupal response (434 transcripts) were also differentially expressed during the early time point (215 transcripts), before mortality diverged in prepupal STR/FTR comparison. This overlap is more than we would expect by chance, based on hypergeometric distribution (p = 1.27E-10). Seventeen of the 434 differentially expressed transcripts (3.9%) overlapped with the late time point (after mortality diverged, 64 transcripts) in prepupae, also more than expected by chance (p = 1.68E-11). Six (1.4%) transcripts differentially expressed in pupae were differentially expressed in both prepupal time points (Fig. 3a).

While differentially expressed transcripts overlap more than expected by chance, when direction of regulation (whether the transcript is up- or down-regulated in FTR-exposed individuals) is considered, all overlap among the three differential expression profiles disappears (Fig. 3b,c). In fact, the only differential expression patterns conserved between the two life stages are regulated in opposite directions (Fig. 3d).

Discussion

Exposure to daily fluctuations in temperature (FTR) during chilling can mitigate the deleterious physiological effects associated chill injury (Colinet et al., 2015). FTR appears to provide a protective benefit across all taxa studied so far, but we lack evidence for a conserved mechanism driving this protective effect. In this study, we exposed developing *M. rotundata* pupae to a static thermal regime (STR), known to lead to chill injury, or to a fluctuating thermal regime (FTR), which diminishes the negative effects of chilling (Bennett et al., 2015). An RNA-seq study after seven days of treatment revealed 434 transcripts that were differentially expressed between the two low temperature treatments. These differentially expressed transcripts provide evidence for cellular damage, oxidative stress, and repair of damage (Table 2, S4). Additionally, we observed a lack of conservation in differential gene expression in response to FTR exposure across life stages in *M. rotundata*, suggesting a robust physiological response driven by variable transcriptional mechanisms.

Membrane imbalance as a driving factor of chill injury

Plants, microbes, and other animals change the physical composition of cell membranes in response to changes in ambient temperature, namely the proportion of unsaturated fatty acids in the phospholipid bilayer (Cossins, 1983). In insects, direct evidence of shifts in membrane phase transitions have yet to be observed (Hayward et al., 2014; Lee, 2010), but strong correlative evidence has been provided (Boardman et al., 2011; Kostál et al., 2006; Kostál et al., 2007; Macmillan et al., 2012). Chill injury in insects has been associated with the collapse of ion gradients presumably caused by damage at the cellular level and possibly resulting in decreased activity of membrane-bound enzymes (Hazel, 1995; MacMillan and Sinclair, 2011) . Extracellular increases of potassium and diminished levels of sodium and magnesium have been observed in chill-injured tropical cockroaches (Kostál, 2004; Kostál et al., 2006; Kostál et al., 2007). These changes in hemolymph (extracellular) ion concentrations could explain the loss of neuromuscular coordination observed in chill-injured insects (Andersen et al., 2016; MacMillan and Sinclair, 2011) and may be a direct effect of damage to cell membranes. In this study, transcripts such as sodium potassium calcium exchanger 6, a mitochondrial potassium-dependent sodium-calcium antiporter (Table 2), are upregulated in individuals exposed to the STR protocol. Mitochondrial function decreases in *Drosophila melanogaster* exposed to constant low temperature (Colinet et al., 2017). Proper mitochondrial function would be heavily dependent on membrane composition, so the differential expression of this sodium potassium calcium exchanger suggests that STR-exposed individuals may be attempting to restore proper ion gradients in response to cellular damage. Additionally, the upregulation of transcripts with GO terms associated with the construction of various cellular components, including cell membranes and integral membrane components (Fig. 2; Table 2), in response to FTR exposure indicates that one of FTR's mechanisms of action is to repair the membrane damage that has accumulated over the duration of low-temperature stress.

The upregulation of aquaporins, a water-selective transmembrane channel, has been observed in freeze-tolerant insects (Philip et al., 2011), and the blockage of those channels has been shown to decrease freeze tolerance due to an inability of the cells to move water out of the cell; subsequently causing damage due to osmotic pressure (Philip et al., 2008). We observed the upregulation of aquaporins during constant low temperature stress (STR); suggesting that these individuals may be attempting to return to proper osmotic conditions. Furthermore, STR-exposed *M. rotundata* showed increased expression of two isoforms

coding for the facilitated trehalose transporter TRET1. This transmembrane protein mediates the movement of trehalose synthesized in the fat body bidirectionally across the cell membrane (Kanamori et al., 2010). The presence of two isoforms for *Tret-1* is consistent with orthologs in *Drosophila melanogaster* (Zhao et al., 2000). The enrichment of *Tret-1* in STR-reared individuals indicates not only changes in membrane composition, but suggests that these individuals may be transporting trehalose into the hemolymph because of its known role as a cryoprotectant (Bale and Hayward, 2010). Interestingly, transcripts coding for a trehalase precursor, an enzyme needed to convert trehalose into glucose (Shukla et al., 2015), and a facilitated glucose transporter (Table 2) were upregulated in FTR-reared individuals, indicating shift in hemolymph composition between the two treatments.

In addition to changes in structural components within membranes, such as aquaporins and trehalose transporters, an increase in unsaturated fatty acids has been observed in response to decreased temperatures across taxa (Cossins, 1983). In our dataset, three different transcripts coding for acyl-delta desaturases, enzymes functioning in the transition between saturated and unsaturated fatty acids, were upregulated in STR-reared individuals relative to FTR (Table 2). The upregulation of transcripts coding for desaturase enzymes has been associated with cold hardiness in the onion maggot, *Delia antiqua* (Kayukawa et al., 2007), indicating this response is conserved. Increased expression of these transcripts suggest that either bees exposed to STR are trying to compensate for a decrease in temperature or that FTR-reared individuals may have less of a strain on their cell membranes due to the temporary increases in temperature.

Antioxidant system activation and repair of damage in the FTR response

Oxidative stress has been implicated in the occurrence of chill injury in many insect species (Joanisse and Storey, 1996; Joanisse and Storey, 1998; Lalouette et al., 2011; Rojas and Leopold, 1996; Torson et al., 2015) and has been hypothesized to be a downstream consequence of membrane phase transitions (Lee, 2010). Quiescent post-wandering *Drosophila melanogaster* larvae exposed to extended low-temperature regimes also show enrichment in transcripts that suggest redox imbalance and possibly oxidative stress (Koštál et al., 2016).

Gene expression indicates that STR-exposed individuals are repairing damage, possibly in response to oxidative stress. The upregulation of a gene coding for a myb domain-containing protein in STR-reared individuals (Table S4) implies that *M. rotundata* is indeed experiencing a stress response. In plant species this class of transcription factors is known to

respond to abiotic stressors, including decreased temperature. The functional unit of the translated proteins are highly conserved implying a similar function in insects (Ambawat et al., 2013). Furthermore, increased expression of *oxidase-peroxidase* (Table S4) is indicative of STR reared individuals experiencing increased levels of peroxide, a consequence of malfunction in mitochondrial respiration (Prasad et al., 1994). If antioxidant systems can't combat the accumulation of free radicals, such as peroxide, damage to cellular structures would be likely.

The upregulation of transcripts in STR-reared bees such as *myofilin isoform b, sestrin-like, and DNA damage-binding protein 1* (Table S4) suggest that STR-exposed individuals experience DNA damage, potentially caused by increased levels of ROS in the bees during chilling. In *Drosophila*, expression levels of sestrins increase in response to target of rapamycin (TOR) under increased levels of ROS (Lee et al., 2010a). The increased expression of this sestrins has also been linked to genotoxic stress including DNA damage (Hay, 2008; Lee et al., 2010b). While sestrins, a class of highly conserved cytoplasmic proteins, have not been shown to repair DNA damage directly, they may be part of a larger signaling cascade. Direct assessments of DNA damage will be required to assess whether oxidative stress may be playing a significant role in the deleterious effects of chill injury or if high levels of antioxidant expression in FTR-exposed individuals is just an artifact of increased metabolic rate due to transient increases in ambient temperature.

Conservation of mechanisms across life stages

In addition to the benefits of FTR observed during pupal development in *M. rotundata*, significant increases in survival have been observed when prepupal post-diapause quiescence are exposed to a similar treatment (Rinehart et al., 2013). For the duration of diapause and post-diapause quiescence in both natural and managed populations, *M. rotundata* are exposed to low temperatures and have mechanisms to cope with these temperatures. Conversely, other life stages, such as developing pupae, which we have assessed in this study, may not be adapted for low temperature exposure and may have different mechanisms driving low temperature stress responses, and subsequently the beneficial effects of FTR. Adult bees observed after STR treatment in both life stages exhibit diminished neuromuscular function, behavior abnormalities, and diminished flight capacity (Bennett et al., 2013; Bennett et al., 2015). These phenotypes suggest chill injury accumulation in both contexts. Initially, we predicted that the temperature stress during the pupal stage would elicit transcriptional responses similar to prepupal responses observed in

Torson *et. al* 2015. This hypothesis was not supported. Markedly different differential expression profiles (Fig. 3) between the two life stages indicates that either 1) the mechanism responsible for a conserved FTR benefit vary throughout development or 2) that the benefit of FTR exposure changes throughout development.

Even within the pupal life stage, temperature exposure can have variable effects on gene expression depending on context. Survival benefits of FTR, relative to STR, are robust to field season (Bennett et al., 2015; Rinehart et al., 2016), but gene expression changes at a finer scale. Expression profiles of the most differentially expressed transcripts identified in this RNA-seq study (Table S2) were not maintained in *M. rotundata* pupae from the following field season (2014, Fig. S2). The direction of regulation, relative to STR, was maintained, but expression was highly variable, even with a doubling of the sample size. High variability between individuals suggests that slight differences in developmental timing are introducing variation or season-specific environmental history influences gene expression, or both. However, it should be noted that the individuals used for qPCR were exposed to one additional month of overwintering prior to pupal development. This short extension of the overwintering period, compared to the RNA-seq individuals, could have also influenced gene expression during subsequent pupal development. Gene expression in response to FTR exposure now appears to be highly context-dependent (i.e., environmental history and developmental stage) and provides further evidence that the conservation of FTR's benefit may not be at the level of gene expression but at a higher level of organization. This result provides the basis for our hypothesis that chill injury repair in response to FTR is a robust physiological response that is driven by life-stage-specific mechanisms.

In biological systems, an animal's ability to maintain a certain characteristic response under perturbations in environmental conditions is known as a robust response (Stelling et al., 2004). With similar physiological responses having been observed across taxa, and, thus far, a lack of evidence of a conserved mechanism at the level of gene expression, we hypothesize that the beneficial effects of chill injury repair during FTR exposure represents a robust physiological response driven by variable gene expression. Redundancy is one basic mechanism of a robust system. Redundancy provides alternative molecular strategies to carry out an action (Hartman et al., 2001). For example, glycosylphosphatidylinositol (GPI)-linked glycoproteins in yeast, termed fungal adhesions, have functionally distinct roles separated temporally and spatially (Guo et al., 2000), but members of this protein family can replace one another when inappropriately expressed in the organism. Similar to our results in *M. rotundata*, work in yeast has shown little overlap in gene expression profiles in response to

stressors (Berry et al., 2011), suggesting that variable downstream effectors (i.e. gene expression response) may enact similar physiological responses (i.e. redundancy or genetic buffering).

Between the larval and pupal life stages in *M. rotundata* a complete restructuring of the animal takes place, resulting in entirely different physiologies. Redundancy in transcript function, or "buffering," may explain why variable gene expression patterns are observed in what appear to be similar physiological response to FTR exposure. However, changes in gene or protein expression and metabolite accumulation might be secondary effects rather than direct or adaptive responses to chilling and/or FTR exposure. As a result of this notion, an alternative hypothesis is that the variable gene expression profiles between life stages in *M. rotundata* is not evidence of different life-stage-specific mechanisms driving the same response at the physiological level, but actually different responses driven by stimuli at a higher level of organization. Additional functional genomic work to identify potentially redundant genes and physiological assays to verify similar physiological responses to FTR exposure will be necessary to provide support for the hypothesis that redundancy allows for conservation of the FTR response across life stages in *M. rotundata*.

Acknowledgements

The authors would like to thank Marnie Larson of the USDA-ARS, Fargo, ND for her technical assistance and advice. We also thank Kendra J. Greenlee of North Dakota State University for her comments on the manuscript.

Competing interest statement

The authors are not aware of any competing interests.

Author contributions

GDY, JPR and AST conceived and designed the research plan. AST analyzed the RNA-seq data. KMK and SAN conducted RT-qPCR validation of RNA-seq results and time series. AST, GDY, and JHB wrote and edited the manuscript. All authors contributed to and approve the content of the final manuscript.

Funding

This research was funded by the United States Department of Agriculture

Data Availability

All raw RNA-seq reads were submitted to the NCBI Sequence read archives (SRA). The SRA BioProject accession number is PRJNA352846.

References

Ambawat, S., Sharma, P., Yadav, N. R. and Yadav, R. C. (2013). MYB transcription factor genes as regulators for plant responses: an overview. *Physiol. Mol. Biol. Plants* **19**, 307–321.

Andersen, M. K., Folkersen, R., MacMillan, H. A. and Overgaard, J. (2016). Cold-acclimation improves chill tolerance in the migratory locust through preservation of ion balance and membrane potential. *J. Exp. Biol.* jeb.150813.

Bale, J. S. and Hayward, S. a L. (2010). Insect overwintering in a changing climate. *J. Exp. Biol.* **213**, 980–994.

Bennett, M. M., Petersen, K., Yocum, G., Rinehart, J., Kemp, W. and Greenlee, K. J. (2013). Effects of extended prepupal storage duration on adult flight physiology of the alfalfa leafcutting bee (Hymenoptera : Megachilidae). *J. Econ. Entomol.* **106**, 1089–1097.

Bennett, M. M., Cook, K. M., Rinehart, J. P., Yocum, G. D., Kemp, W. P. and Greenlee, K. J. (2015). Exposure to suboptimal temperatures during metamorphosis reveals a critical developmental window in the solitary bee, *Megachile rotundata*. *Physiol. Biochem. Zool.* **88**, 508–520.

Berry, D. B., Guan, Q., Hose, J., Haroon, S., Gebbia, M., Heisler, L. E., Nislow, C., Giaever, G. and Gasch, A. P. (2011). Multiple means to the same end: the genetic basis of acquired stress resistance in yeast. *PLoS Genet.* **7**, e1002353.

Boardman, L., Terblanche, J. S. and Sinclair, B. J. (2011). Transmembrane ion distribution during recovery from freezing in the woolly bear caterpillar *Pyrrharctia isabella* (Lepidoptera: Arctiidae). *J. Insect Physiol.* **57**, 1154–1162.

Boardman, L., Sorensen, J. G. and Terblanche, J. S. (2013). Physiological responses to fluctuating thermal and hydration regimes in the chill susceptible insect, *Thaumatotibia leucotreta*. *J. Insect Physiol.* **59**, 781–794.

Chen, H. and Boutros, P. C. (2011). VennDiagram: a package for the generation of highly-customizable Venn and Euler diagrams in R. *BMC Bioinformatics* **12**, 35.

Chen, C. P. and Denlinger, D. L. (1992). Reduction of cold injury in flies using an intermittent pulse of high temperature. *Cryobiology* **29**, 138–143.

Colinet, H., Renault, D., Hance, T. and Vernon, P. (2006). The impact of fluctuating thermal regimes on the survival of a cold-exposed parasitic wasp, *Aphidius*

colemani. *Physiol. Entomol.* **31**, 234–240.

Colinet, H., Hance, T., Vernon, P., Bouchereau, A. and Renault, D. (2007). Does fluctuating thermal regime trigger free amino acid production in the parasitic wasp *Aphidius colemani* (Hymenoptera: Aphidiinae). *Comp. Biochem. Physiol. A. Mol. Integr. Physiol.* **147**, 484–492.

Colinet, H., Lalouette, L. and Renault, D. (2011). A model for the time–temperature–mortality relationship in the chill-susceptible beetle, *Alphitobius diaperinus*, exposed to fluctuating thermal regimes. *J. Therm. Biol.* **36**, 403–408.

Colinet, H., Sinclair, B. J., Vernon, P. and Renault, D. (2015). Insects in fluctuating thermal environments. *Annu. Rev. Entomol.* **60**, 123–140.

Colinet, H., Renault, D. and Roussel, D. (2017). Cold acclimation allows *Drosophila* flies to maintain mitochondrial functioning under cold stress. *Insect Biochem. Mol. Biol.* **80**, 52–60.

Conesa, A., Götz, S., García-Gómez, J. M., Terol, J., Talón, M. and Robles, M. (2005). Blast2GO: a universal tool for annotation, visualization and analysis in functional genomics research. *Bioinformatics* **21**, 3674–3676.

Cossins, A. R. (1983). *Cellular Acclimation to Environmental Change*. (ed. Cossins, A. R.) and Sheterline, P.) Cambridge: Cambridge University Press.

Easterling, D. R., Meehl, G. A., Parmesan, C., Changnon, S. A., Karl, T. R. and Mearns, L. O. (2000). Climate extremes: observations, modeling and impacts. *Science.* **289**, 2068–2074.

Guo, B., Styles, C. a, Feng, Q. and Fink, G. R. (2000). A *Saccharomyces* gene family involved in invasive growth, cell-cell adhesion, and mating. *Proc. Natl. Acad. Sci. U. S. A.* **97**, 12158–12163.

Hansen, J., Sato, M. and Ruedy, R. (2012). Perception of climate change. *Proc. Natl. Acad. Sci. U. S. A.* **109**, E2415–E2423.

Hartman, J. L., Garvik, B., Hartwell, L., Iv, J. L. H., Garvik, B. and Hartwell, L. (2001). Principles for the buffering of genetic variation. *Science.* **291**, 1001–1004.

Hay, N. (2008). p53 Strikes mTORC1 by Employing Sestrins. *Cell Metab.* **8**, 184–185.

Hayward, S. A. L., Manso, B. and Cossins, A. R. (2014). Molecular basis of chill resistance adaptations in poikilothermic animals. *J. Exp. Biol.* **217**, 6–15.

Hazel, J. R. (1995). Thermal adaptation in biological membranes: Is homeoviscous adaptation the explanation. *Annu. Rev. Physiol.* **57**, 19–42.

Jing, X.-H., Wang, X.-H. and Kang, L. (2005). Chill injury in the eggs of the migratory locust, *Locusta migratoria* (Orthoptera: Acrididae): the time-temperature relationship with high-temperature interruption. *Insect Sci.* 171–178.

Joanisse, D. and Storey, K. (1996). Oxidative stress and antioxidants in overwintering larvae of cold-hardy goldenrod gall insects. *J. Exp. Biol.* **199**, 1483–1491.

Joanisse, D. R. and Storey, K. B. (1998). Oxidative stress and antioxidants in stress and recovery of cold-hardy insects. *Insect Biochem. Mol. Biol.* **28**, 23–30.

Kanamori, Y., Saito, A., Hagiwara-Komoda, Y., Tanaka, D., Mitsumasu, K., Kikuta, S., Watanabe, M., Cornette, R., Kikawada, T. and Okuda, T. (2010). The trehalose transporter 1 gene sequence is conserved in insects and encodes proteins with different kinetic properties involved in trehalose import into peripheral tissues. *Insect Biochem. Mol. Biol.* **40**, 30–37.

Kanehisa, M., Goto, S., Sato, Y., Furumichi, M. and Tanabe, M. (2012). KEGG for integration and interpretation of large-scale molecular data sets. *Nucleic Acids Res.* **40**, D109-114.

Kayukawa, T., Chen, B., Hoshizaki, S. and Ishikawa, Y. (2007). Upregulation of a desaturase is associated with the enhancement of cold hardiness in the onion maggot, *Delia antiqua*. *Insect Biochem. Mol. Biol.* **37**, 1160–1167.

Kostál, V. (2004). On the nature of pre-freeze mortality in insects: water balance, ion homeostasis and energy charge in the adults of *Pyrrhocoris apterus*. *J. Exp. Biol.* **207**, 1509–1521.

Kostál, V. (2006). Eco-physiological phases of insect diapause. *J. Insect Physiol.* **52**, 113–127.

Kostál, V., Yanagimoto, M. and Bastl, J. (2006). Chilling-injury and disturbance of ion homeostasis in the coxal muscle of the tropical cockroach (*Nauphoeta cinerea*). *Comp. Biochem. Physiol. B. Biochem. Mol. Biol.* **143**, 171–179.

Kostál, V., Renault, D., Mehrabianová, A. and Bastl, J. (2007). Insect cold tolerance and repair of chill-injury at fluctuating thermal regimes: role of ion homeostasis. *Comp. Biochem. Physiol. A. Mol. Integr. Physiol.* **147**, 231–238.

Kostál, V., Korbelová, J., Štětina, T., Poupardin, R., Colinet, H., Zahradníčková, H., Opekarová, I., Moos, M. and Šimek, P. (2016). Physiological basis for low-temperature survival and storage of quiescent larvae of the fruit fly *Drosophila melanogaster*. *Sci. Rep.* **6**, 32346.

Lalouette, L., Williams, C. M., Hervant, F., Sinclair, B. J. and Renault, D. (2011). Metabolic rate and oxidative stress in insects exposed to low temperature thermal fluctuations. *Comp. Biochem. Physiol. A. Mol. Integr. Physiol.* **158**, 229–234.

Lee, R. E. (2010). *Low Temperature Biology of Insects*. (ed. Denlinger, D. L.) and Lee, R. E.) Cambridge, NY: Cambridge University Press.

Lee, J. H., Budanov, A. V, Park, E. J., Birse, R., Kim, T. E., Perkins, G. A., Ocorr, K., Ellisman, M. H., Bodmer, R., Bier, E., et al. (2010a). Sestrin as a feedback inhibitor of TOR that prevents age-related pathologies. *Science.* **327**, 1223–1228.

Lee, J. H., Bodmer, R., Bier, E. and Karin, M. (2010b). Sestrins at the crossroad between stress and aging. *Aging.* **2**, 369–374.

Leopold, R. A., Rojas, R. R. and Atkinson, P. W. (1998). Post pupariation cold storage of three species of flies: increasing chilling tolerance by acclimation and recurrent recovery periods. *Cryobiology* **36**, 213–224.

Macmillan, H. A., Williams, C. M., Staples, J. F. and Sinclair, B. J. (2012). Reestablishment of ion homeostasis during chill-coma recovery in the cricket *Gryllus pennsylvanicus*. *Proc. Natl. Acad. Sci. U. S. A.* **109**, 20750–20755.

MacMillan, H. a and Sinclair, B. J. (2011). The role of the gut in insect chilling injury: cold-induced disruption of osmoregulation in the fall field cricket, *Gryllus pennsylvanicus*. *J. Exp. Biol.* **214**, 726–734.

MacRae, T. H. (2010). Gene expression, metabolic regulation and stress tolerance during diapause. *Cell. Mol. Life Sci.* **67**, 2405–2424.

Marshall, K. E. and Sinclair, B. J. (2012). The impacts of repeated cold exposure on insects. *J. Exp. Biol.* **215**, 1607–1613.

Nedvěd, O., Lavy, D. and Verhoef, H. A. (1998). Modelling the time-temperature relationship in cold injury and effect of high-temperature interruptions on survival in a chill-sensitive collembolan. *Funct. Ecol.* **12**, 816–824.

O'Neill, K. M., O'Neill, R. P., Kemp, W. P. and Delphia, C. M. (2011). Effect of temperature on post-wintering development and total lipid content of alfalfa leafcutting bees. *Environ. Entomol.* **40**, 917–930.

Philip, B. N., Yi, S.-X., Elnitsky, M. A. and Lee, R. E. (2008). Aquaporins play a role in desiccation and freeze tolerance in larvae of the goldenrod gall fly, *Eurosta solidaginis*. *J. Exp. Biol.* **211**, 1114–1119.

Philip, B. N., Kiss, A. J. and Lee, R. E. (2011). The protective role of aquaporins in the

freeze-tolerant insect *Eurosta solidaginis*: functional characterization and tissue abundance of EsAQP1. *J. Exp. Biol.* **214**, 848–857.

Prasad, T. K., Anderson, M. D., Martin, B. A. and Stewart, C. R. (1994). Evidence for chilling-induced oxidative stress in maize seedlings and a regulatory role for hydrogen peroxide. *Plant Cell* **6**, 65–74.

Renault, D., Nedved, O., Hervant, F. and Veron, P. (2004). The importance of fluctuating thermal regimes for repairing chill injuries in the tropical beetle *Alphitobius diaperinus* (Coleoptera : Tenebrionidae) during exposure to low temperature. *Physiol. Entomol.* **29**, 139–145.

Rinehart, J. P., Yocum, G. D., West, M. and Kemp, W. P. (2011). A fluctuating thermal regime improves survival of cold-mediated delayed emergence in developing *Megachile rotundata* (Hymenoptera: Megachilidae). *J. Econ. Entomol.* **104**, 1162–1166.

Rinehart, J. P., Yocum, G. D., Kemp, W. P. and Greenlee, K. J. (2013). A fluctuating thermal regime improves long-term survival of quiescent prepupal *Megachile rotundata* (Hymenoptera : Megachilidae). *Apic. Soc. insects* **106**, 1081–1088.

Rinehart, J. P., Yocum, G. D., Kemp, W. P. and Bowsher, J. H. (2016). Optimizing fluctuating thermal regime storage of developing *Megachile rotundata* (Hymenoptera: Megachilidae). *J. Econ. Entomol.* **109**, 993–1000.

Rojas, R. R. and Leopold, R. A. (1996). Chilling injury in the housefly: evidence for the role of oxidative stress between pupariation and emergence. *Cryobiology* **33**, 447–458.

Shukla, E., Thorat, L. J., Nath, B. B. and Gaikwad, S. M. (2015). Insect trehalase: physiological significance and potential applications. *Glycobiology* **25**, 357–367.

Stanzione, D. (2011). The iPlant collaborative: cyberinfrastructure to feed the world. *Computer (Long. Beach. Calif).* **44**, 44–52.

Stelling, J., Sauer, U., Szallasi, Z., Doyle, F. J. and Doyle, J. (2004). Robustness of cellular functions. *Cell* **118**, 675–685.

Torson, A. S., Yocum, G. D., Rinehart, J. P., Kemp, W. P. and Bowsher, J. H. (2015). Transcriptional responses to fluctuating thermal regimes underpinning differences in survival in the solitary bee *Megachile rotundata*. *J. Exp. Biol.* **218**, 1060–1068.

Trapnell, C., Roberts, A., Goff, L., Pertea, G., Kim, D., Kelley, D. R., Pimentel, H., Salzberg, S. L., Rinn, J. L. and Pachter, L. (2012). Differential gene and transcript

expression analysis of RNA-seq experiments with TopHat and Cufflinks. *Nat. Protoc.* **7**, 562–578.

Vandesompele, J., De Preter, K., Pattyn, F., Poppe, B., Van Roy, N., De Paepe, A. and Speleman, F. (2002). Accurate normalization of real-time quantitative RT-PCR data by geometric averaging of multiple internal control genes. *Genome Biol.* **3**, RESEARCH0034.1.

Vasseur, D. A., Delong, J. P., Gilbert, B., Greig, H. S., Harley, C. D. G., Mccann, K. S., Savage, V., Tunney, T. D., Connor, M. I. O., Delong, J. P., et al. (2014). Increased temperature variation poses a greater risk to species than climate warming Increased temperature variation poses a greater risk to species than climate warming. *Proc. Biol. Sci.* **281**, 20132612.

Whitfield, G. H. and Richards, K. W. (1992). Temperature dependent development and survival of immature stages of the alfalfa leafcutter bee, *Megachile rotundata* (Hymenoptera: Megachilidae). *Apidologie* **23**, 11–23.

Winston, P. W. and Bates, D. H. (1960). Saturated solutions for the control of humidity in biological research. *Ecology* **41**, 232–237.

Yocum, G. D., Žďárek, J., Joplin, K. H., Lee, R. E., Smith, D. C., Manter, K. D. and Denlinger, D. L. (1994). Alteration of the eclosion rhythm and eclosion behavior in the flesh fly, *Sarcophaga crassipalpis*, by low and high temperature stress. *J. Insect Physiol.* **40**, 13–21.

Yocum, G. D., Kemp, W. P., Bosch, J. and Knoblett, J. N. (2006). Thermal history influences diapause development in the solitary bee *Megachile rotundata*. *J. Insect Physiol.* **52**, 1113–1120.

Yocum, G. D., Rinehart, J. P. and Kemp, W. P. (2012). Duration and frequency of a high temperature pulse affect survival of emergence-ready *Megachile rotundata* (Hymenoptera: Megachilidae) during low-temperature incubation. *J. Econ. Entomol.* **105**, 14–19.

Zhao, Q., Spradling, A. C., Mattei, B., An, H. J., Weinstock, G. M., Holt, R. A., Zheng, L., Harris, M., Ke, Z., Zaveri, J. S., et al. (2000). The genome sequence of *Drosophila melanogaster*. *Science.* **287**, 2185—2195.

Figures

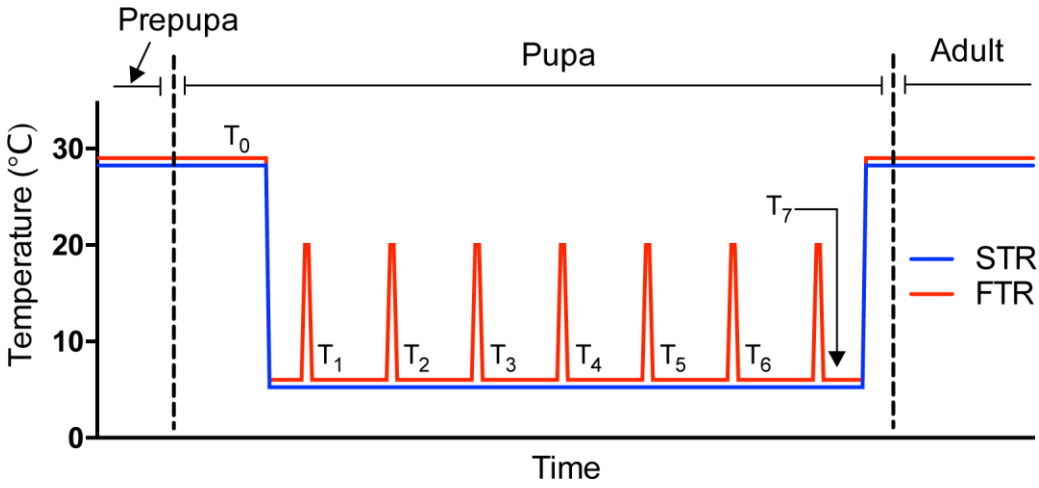

Figure 1: Temperature Regimes and RNA collection time points. *M. rotundata* were reared at 29°C until "red-eye" pigmentation stage during pupal development. Individuals were exposed to either an STR of 6°C or an FTR of 6°C with a one hour pulse to 20°C with one-hour ramp up and ramp down times. RNA was harvested at T_7 for the RNA-seq and T_0-T_7 for the qPCR time series.

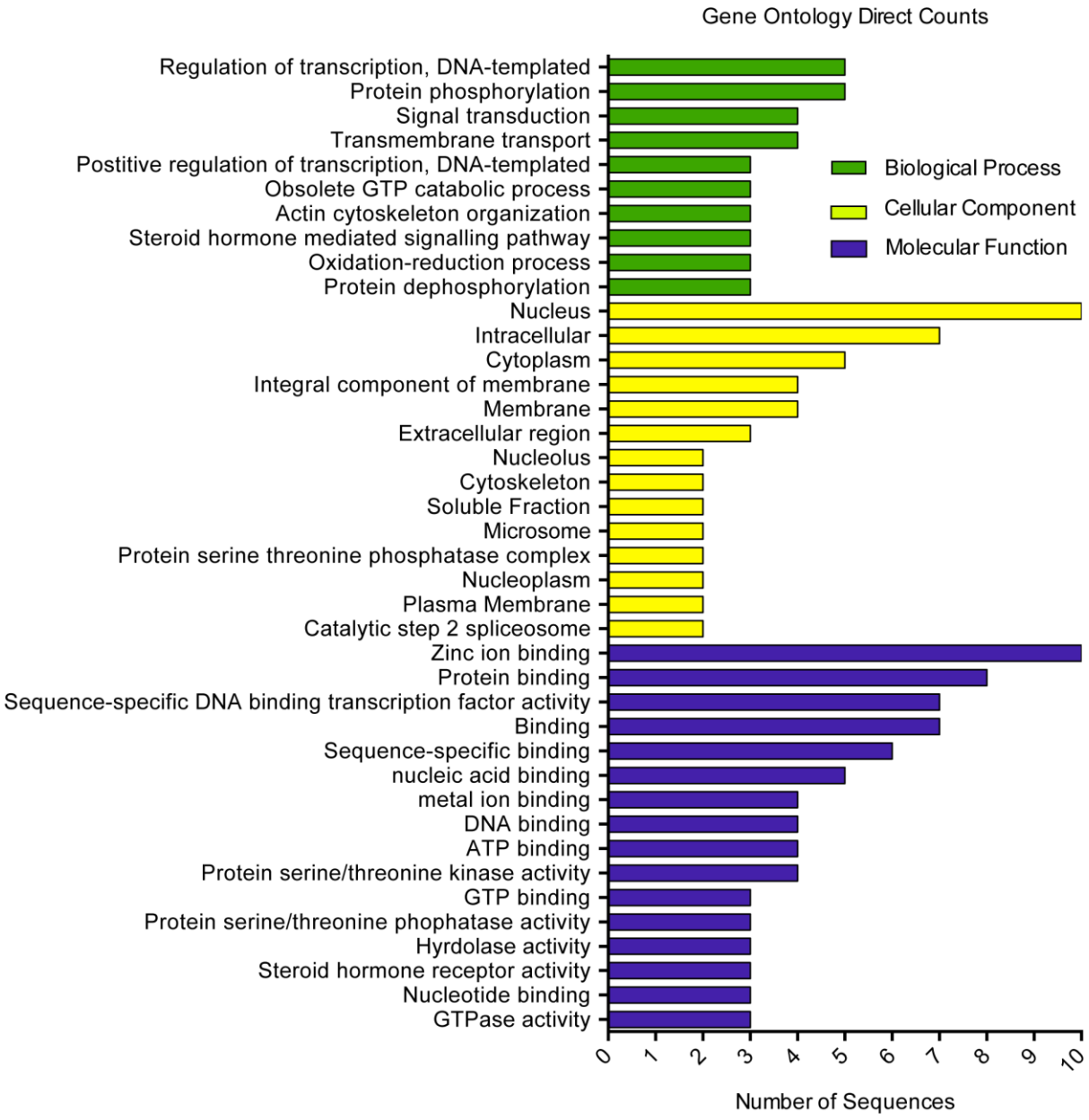

Figure 2: Gene ontology of transcripts upregulated in FTR. Most prominent GO terms for biological processes, molecular function, and cellular components of transcripts upregulated in *M. rotundata* exposed to FTR for seven days.

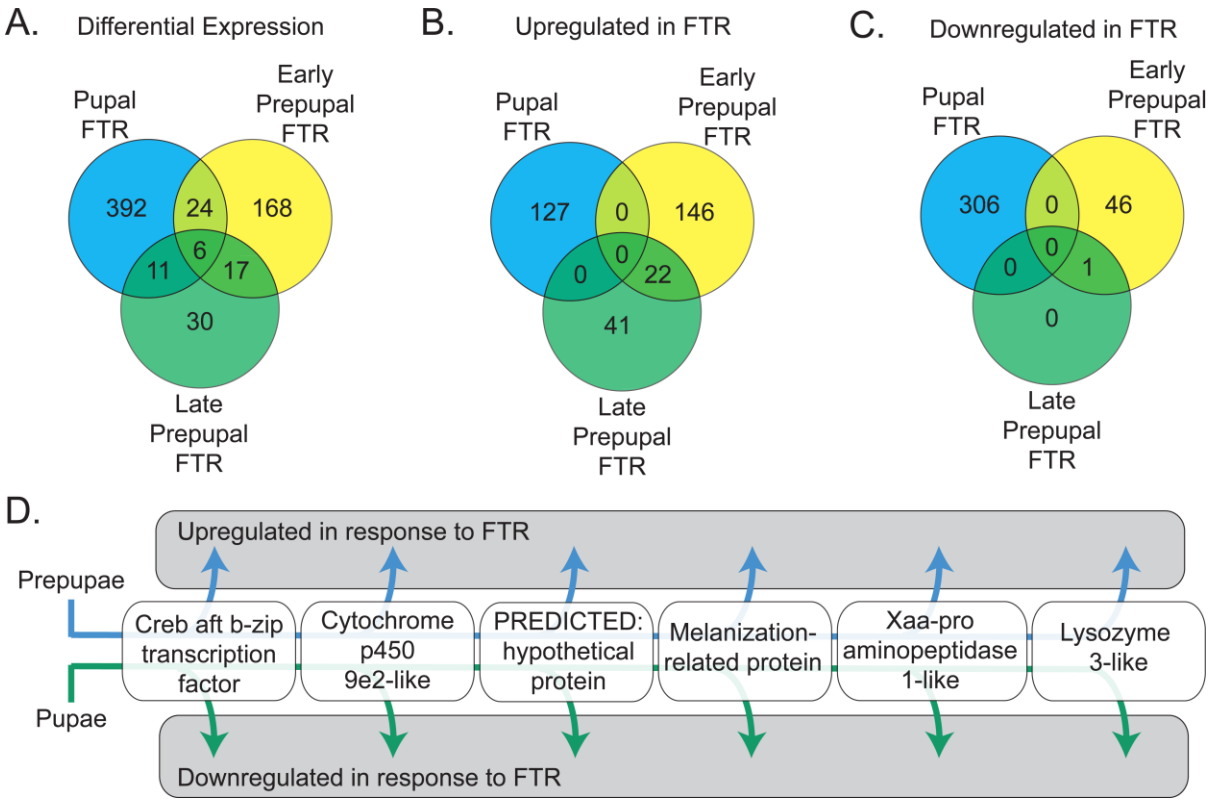

Figure 3: Comparison of differential expression profiles of pupa and post-diapause quiescent prepupa exposed to FTR treatment. The differential expression profiles in this study (interrupted development) were compared to two time points sampled during long term FTR treatment during the prepupal life stage (Torson et al., 2015). A) Comparison of differentially expressed transcripts; B) Transcripts upregulated in FTR; C) Transcripts downregulated in FTR; D) Graphical representation of the direction of regulation of the six shared transcripts from panel A.

Tables

Table 1. Each paired-end (PE) read RNA-seq library was mapped against the *M. rotundata* genome. Each treatment contained three biological replicates

Biological Replicate	Total Reads	Mapped Reads	Overall read alignment	Concordant pair alignment
STR_1	42,661,992	29,877,839	70.0%	65.8%
STR_2	43,529,948	28,940,759	66.5%	61.9%
STR_3	36,809,014	25,976,650	70.6%	66.3%
FTR_1	65,929,382	46,612,625	69.2%	64.5%
FTR_2	48,182,900	33,471,363	69.5%	64.7%
FTR_3	46,562,730	32,100,944	68.9%	64.6%
Average:	47,279,330	32,830,030	69.11%	64.5%

Table 2. Candidate genes involved in cell membrane structure and function. Fold change is $\log_2$ transformed and relative to FTR. A negative fold change (grey rows) is an upregulation in STR. The Gene Ontology (GO) terms used for inclusion into this table are Integral membrane component (IMC), Membrane transport (MT), Transmembrane signaling (TS), IH (Ion homeostasis), Cell membrane (CM), and Receptor Activity (RA).

Transcript ID	GO Term	Transcript	Fold Change
MROT_00006513	IMC, MT	aquaporin -like	-2.42146
MROT_00001868	IMC, TS	green-sensitive opsin-like	-2.18108
MROT_00006341	IMC	dusky cg9355-pa	-2.13892
MROT_00003036	IMC, TS	isoform b	-2.13224
MROT_00008924	IMC	heparan sulfate 2-o-sulfotransferase	-1.96306
MROT_00010957	IMC	acyl- delta desaturase	-1.94342
MROT_00011033	IMC, TS	toll-like receptor 1	-1.87515
MROT_00004594	IMC, MT	protein patched	-1.78456
MROT_00007828	IMC, MT	sodium potassium calcium exchanger 6	-1.68664
MROT_00006050	IH	transferrin	-1.6421
MROT_00005087	CM, MT	sodium dicarboxylate	-1.55519
MROT_00000476	IMC	tetraspanin isoform b	-1.54449
MROT_00002329	IMC	elongation of very long chain fatty acids protein aael008004-like	-1.52267
MROT_00002610	IMC, MT	facilitated trehalose transporter tret1-like	-1.49314
MROT_00009520	IMC, MT	solute carrier family 17 member 9-like	-1.43109
MROT_00009446	IMC	slit homolog 1	-1.42611
MROT_00005368	CM, MT	inorganic phosphate cotransporter-like	-1.4077
MROT_00010592	CM, TS	fibrillin-2 isoform x3	-1.38474
MROT_00010666	IMC, TS	protein jagged-1	-1.22979
MROT_00010168	IMC, MT	facilitated trehalose transporter tret1-like	-1.21413
MROT_00008614	IMC	n-acetylgalactosaminyltransferase 7	-1.20159
MROT_00008401	IMC	acyl- delta desaturase-like	-1.17683
MROT_00003003	IMC, MT	aquaporin	-1.13869
MROT_00000939	CM	stromal cell-derived factor 2	-1.09454
MROT_00008284	IMC, TS	adenylate cyclase type 2-like	-1.07231
MROT_00005713	IMC, RA	progestin and adipoq receptor family member 3-like	-1.06359
MROT_00005193	IMC	cg34114 cg34114-pb	-1.05511
MROT_00007187	IMC	atp-binding cassette sub-family g member 1-like	-1.04225
MROT_00003345	CM, TS	abc transporter g family member 22-like	-1.00873
MROT_00003491	IMC, RA	translocon-associated protein subunit beta	-0.974473
MROT_00007021	CM, RA	protein croquemort	-0.929458
MROT_00008406	IMC	acyl- delta desaturase	-0.807356
MROT_00002239	IMC, MT	solute carrier family facilitated glucose transporter member 1	0.759531
MROT_00003829	IMC, MT	synaptic vesicle protein	0.83321
MROT_00001571	IMC	trehalase precursor	0.981384
MROT_00008195	IMC, MT	mitochondrial glutamate	1.16316
MROT_00001219	IH	mucolipin-3	1.2947
MROT_00008103	IMC	osiris 14	2.07664

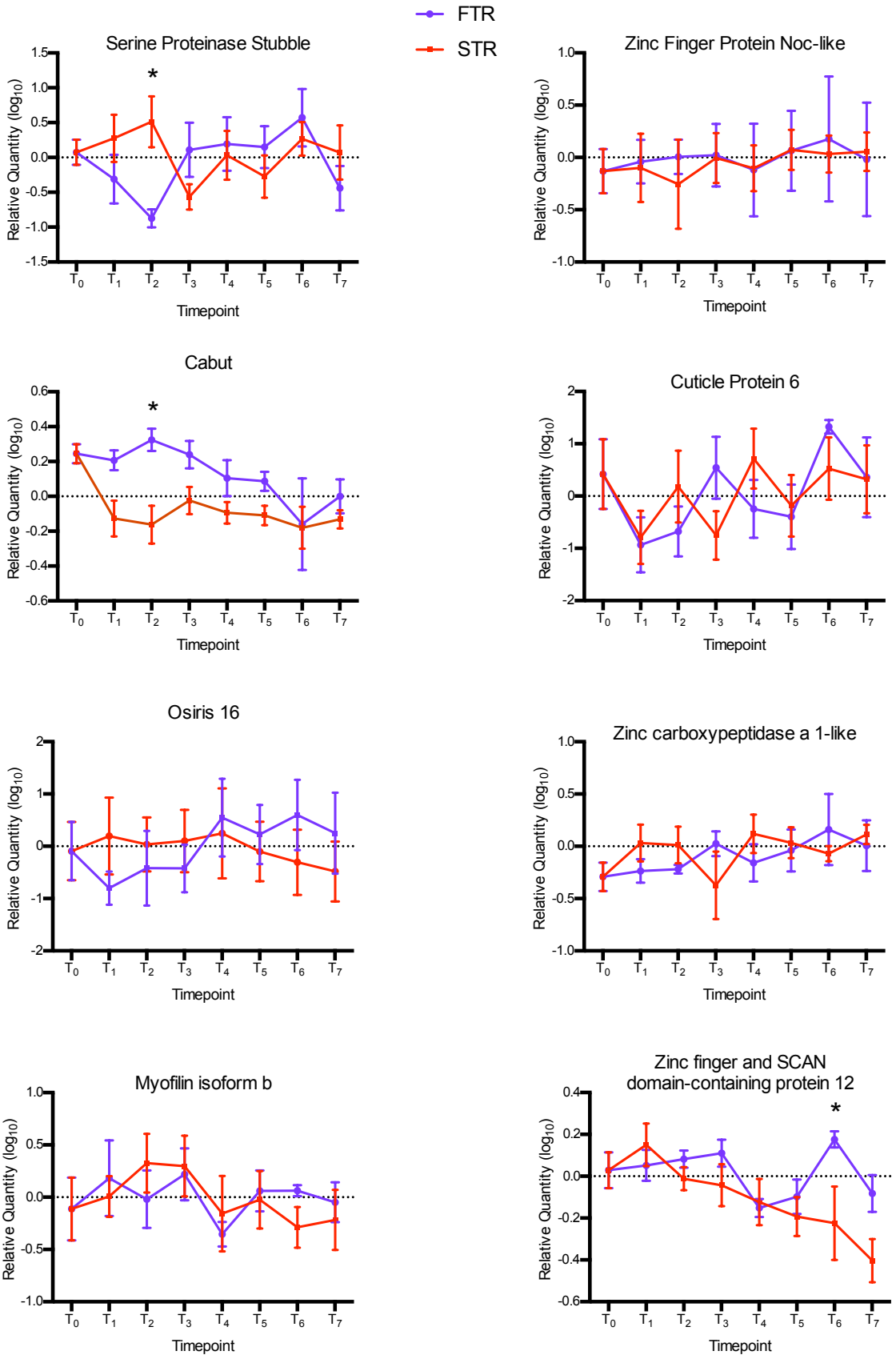

Journal of Experimental Biology • Supplementary information

Figure S1: Biological function gene ontology of differentially expressed transcripts after seven days of low temperature stress.

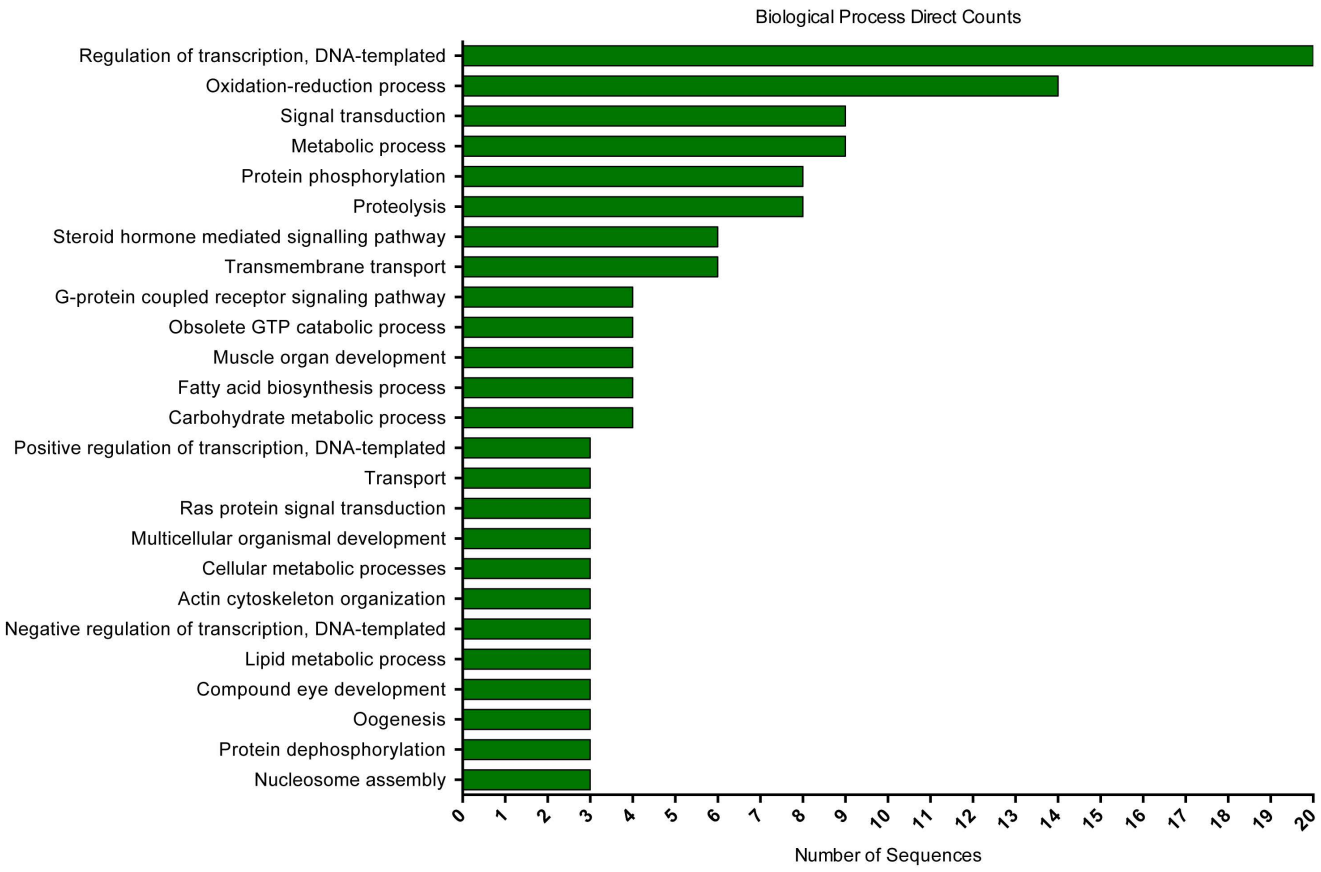

Figure S2: Expression profiles of candidate genes during temperature stress. The expression of candidate genes identified in the RNA-seq analysis was assessed throughout the entire duration of low temperature stress after extended overwintering (n=6). The data are presented as mean ± s.e.m. Asterisks indicate a significant difference in expression between STR and FTR determined by ANOVA.

Table S1. qPCR validation primers. Primer sets highlighted in grey were reference gene candidates.

Transcript ID	Forward	Reverse
MROT_00009775 Set 1	CGA AAC GCT CGC TTA CAA ATA G	CAT TGA GGT GGC TCG TAT CTC
MROT_00009775 Set 2	CCT CAG AGA CAT GAA GGA ACA C	GTG GGA AGA ACT GGG TGA TAT G
MROT_0000590 Set 1	AAT GAG CCT ACG GAA AGA AGA G	GCT TTG GTG CTA GAG GAT GT
MROT_0000590 Set 2	TCG TGC CCT TAC AAA GAC TG	CGA ACT TCT TCT CTC CGG TAT G
MROT_00008799 Set 1	GAC CTG AAC CGA CGT CTT TAA T	CAG TTG ACT CAC AGA GGA GAA C
MROT_00008799 Set 2	CTC CTG GGA ATC AGA TGG TTA G	GGC TTG AAC TCC GCT GAT AA
MROT_00010646 Set 1	GCC GAT ACG ATT GTG AGA GAG	GTT CCA TGT TGG TTC CGT TTC
MROT_00010646 Set 2	ACG CGA GAG GAA CAA CAT AG	GTC GTT GTC CTT CAC CAG AA
MROT_00008869 Set 1	TGC CAA CCA ACA CAA GGA	AGC TAC CGG TTT GCC ATA TT
MROT_00008869 Set 2	CAA AGC CAC AGC ACA CAT TC	ATC GCG ATG ATC TCT GGT TG
MROT_00005226 Set 1	GGC AAA GGG AAT GAC ACT TG	GAG TAC ACA TTC ACA ATC CAT GAG
MROT_00005226 Set 2	CCA ATG GAT GAA TGC CAG AAA T	GAG AAC AAG TGT CAT TCC CTT TG
MROT_00008103 Set 1	GGT CGT GCC AAG ATC AAG AA	CTT AGG CTT CCG AGG ATG ATT G
MROT_00008103 Set 2	CAA TCA TCC TCG GAA GCC TAA G	GCC GAA CAA CCT CTG GAA A
MROT_00002094 Set 1	TGT GAG ATT GGA TGC GAA GAA	CAA CGA GCC TAG CAG AGA TTT A
MROT_00002094 Set 2	GCA TCG GGC AAC AAA TCT TC	CAC GAC TCG TAC GGC TTA AA
MROT_00008639 Set 1	GTG TGG TTA GCA GTT CAG TAG AG	GAA TTT GGC CTT CCT TGT GAT G
MROT_00008639 Set 2	GTT ACG TCC GAG CCT TGA AA	GAG GAA TGC AGC TCA GGA TAA T
MROT_00004919 Set 1	ACA ACC CAC AAC CAG AAG AG	TTC CAC TGT GCA CAT CGT ATT A
MROT_00004919 Set 2	GAG GAG AAT GGC GAT CAC TAA A	CTT CCC TTC GTA GCG TTT CT
MROT_00001385 Set 1	CCA GTT GGT GTT CGA GGA ATA G	TGC TCC AAG TCC AGT GTT ATG
MROT_00002467 Set 1	TAC CTC CTC CTC CGA CTT TAC	CTG GCC GTC CGC ATT ATT A
MROT_00003376 Set 1	CTG GAC CAA AGC AAC AAA CG	CTG GGC CTG TAT CTT CTT CTT C
MROT_00003926 Set 1	GGA GGC GAT CCT ACA AAT ACT G	GTC TAC CTC GAC TTT CTC AAT CG
MROT_0000714 Set 1	CAG TAC ATG CTT TGG CGT TAT G	CCA GAA TCT CCT GTT TCT CCT G
MROT_0000812 Set 1	AGC AGA GAA GAA GAC GAG AAA C	GTG CAG CAG TAC GAC CAA TA
MROT_00008586 Set 1	TGA AAG CTT CTG CGG CTA TTA	CCA ACT TCT GTC TGG TCT CTT C
MROT_00009058 Set 1	GAT GGC AAA CAA GCT AGA AGA AC	GGC TGA TAG AGC AAC GAA CA

Table S2. Ten most up- and down-regulated transcripts after treatment. Log_2 fold change relative to FTR. A negative fold change is an upregulation in STR.

Transcript ID	Sequence Description	Fold Change (log_2)
MROT_00006789	cuticle protein 6	-8.56374
MROT_00008105	osiris 16	-8.42492
MROT_00010933	PREDICTED: uncharacterized protein LOC100879602	-7.38722
MROT_00010985	leucine-rich repeat-containing g-protein coupled receptor 4-like	-6.34828
MROT_00007545	zinc carboxypeptidase a 1-like	-5.2878
MROT_00002812	carboxypeptidase b	-4.91085
MROT_00002813	trypsin-1	-4.91085
MROT_00001862	heavy metal-translocating p-type atpase	-4.42962
MROT_00002788	PREDICTED: hypothetical protein LOC100741758	-4.41335
MROT_00008052	cuticle collagen 3a3	-4.35375
MROT_00009775	tbc1 domain family member 4-like	1.71071
MROT_00005906	cabut	1.72365
MROT_00008799	zinc finger SCAN domain containing protein	1.78574
MROT_00010646	ccaat enhancer-binding protein	1.87841
MROT_00008869	actin-binding rho-activating isoform 1	2.04768
MROT_00005226	seminal fluid protein hacp027	2.07091
MROT_00008103	osiris 14	2.07664
MROT_00002094	zinc finger protein noc-like	2.26969
MROT_00008639	myofilin isoform b	2.33654
MROT_00004919	protein argonaute-2	3.67798

Table S3. qPCR validation. Yellow indicates transcripts that were validated with one primer set and green indicates those validated with two. Genes identified as non-differentially expressed were those used to determine stable reference genes.

Transcript ID	Differentially Expressed in RNA-seq	qPCR Validated
MROT_00009775	Yes	Yes
MROT_00005906	Yes	Yes
MROT_00008799	Yes	Yes
MROT_00010646	Yes	No
MROT_00008869	Yes	Yes
MROT_00005226	Yes	Yes
MROT_00008103	Yes	No
MROT_00002094	Yes	Yes
MROT_00008639	Yes	Yes
MROT_00004919	Yes	Yes
MROT_00001385	No	Yes
MROT_00002467	No	Yes
MROT_00003376	No	Yes
MROT_00003926	No	Yes
MROT_00007147	No	No
MROT_00008127	No	Yes
MROT_00008586	No	Yes
MROT_00009058	No	No

Table S4: Gene ontology of non-cell-membrane transcripts. Log_2 fold change relative to FTR. A negative fold change (grey rows) is an upregulation in STR.

Transcript ID	Function	Transcript	Fold Change
MROT_00000137	Apoptotic Process	death associated protein	-1.04078
MROT_00007022	Apoptotic Process	intraflagellar transport protein 57 homolog	-1.06966
MROT_00004114	Developmental Process	homeobox protein	1.25495
MROT_00005807	Developmental Process	udp-glucose 6-dehydrogenase	1.17127
MROT_00002687	Developmental Process	ras association domain-containing protein 8-like	0.808743
MROT_00006453	Developmental Process	e3 ubiquitin-protein ligase su -like	0.799208
MROT_00010835	Developmental Process	paired box protein pax-2-b	-0.916377
MROT_00000481	Developmental Process	ecdysone-induced protein 78c	-1.30957
MROT_00008639	DNA repair	myofilin isoform b	2.33654
MROT_00004041	DNA repair	dna damage-binding protein 1	1.02919
MROT_00007044	DNA repair	p53 regulated pa26 nuclear protein	0.797203
MROT_00004541	DNA repair	meiotic recombination 11	-1.27712
MROT_00008401	Oxidation-reduction	acyl- delta desaturase-like	-1.17683
MROT_00010957	Oxidation-reduction	acyl- delta desaturase	-1.94342
MROT_00003853	Neurogenesis	isoform b	0.860505
MROT_00004354	Neurogenesis	storkhead-box protein 1	-0.726152
MROT_00002967	Neurogenesis	kn motif and ankyrin repeat domain-containing protein 1	-0.802562
MROT_00007176	Neurogenesis	peptidylglycine alpha-hydroxylating monooxygenase	0.996843
MROT_00007352	Oxidation/reduction	cytochrome b5-related protein	-0.85795
MROT_00000322	Oxidation/reduction	fatty acyl- reductase cg5065-like	-0.954789
MROT_00001392	Oxidation/reduction	probable cytochrome p450 305a1	-1.11015
MROT_00002750	Oxidation/reduction	1-cys peroxiredoxin	-1.35647
MROT_00005092	Oxidation/reduction	d-3-phosphoglycerate dehydrogenase	-1.57624
MROT_00007629	Oxidation/reduction	homogentisate -dioxygenase	-1.57882
MROT_00009098	Oxidation/reduction	pro-phenol oxidase subunit 2	-1.712
MROT_00008416	Oxidation/reduction	cytochrome p450 mitochondrial	-1.73091
MROT_00008044	Oxidation/reduction	oxidase peroxidase	-2.22979
MROT_00009438	Oxidation/reduction	10-formyltetrahydrofolate dehydrogenase	-2.33033
MROT_00003522	Oxidation/reduction	glyoxylate reductase hydroxypyruvate reductase	-2.36061
MROT_00008221	Oxidation/reduction	short-chain dehydrogenase	-2.41981
MROT_00010247	Oxidation/reduction	cytochrome p450 6b1-like	-2.44822

MROT_00000691	Oxidation/reduction	retinol dehydrogenase 14	-2.57532
MROT_00008095	Oxidation/reduction	osiris 2 cg1148-pb	-3.3388
MROT_00000580	Oxidation/reduction	fatty acid synthase	-4.00072
MROT_00000146	Oxidation/reduction	protein kintoun-like	1.41663
MROT_00008499	Oxidation/reduction	cytochrome p450 4g15	-2.2377
MROT_00002050	Stress response	myb domain-containing protein	-2.08356

Supplementary Results

qPCR time series:

Expression a subset of the most significantly up- and down-regulated transcripts in the RNA-seq study after seven days of treatment (Table S2) was assessed across the duration of low temperature stress (Fig. 1) using qPCR. Generally, direction of regulation between treatments at T_7 was maintained between this time series (different field season) and the RNA-seq time point, but the qPCR time series had greater in expression between biological replicates within treatment and time point resulting in a lack of statistical significance even after sample sizes were increased from three to six. Expression of the transcript coding for a zinc finger SCAN domain containing protein had a significant time effect ($F_{7, 70} = 3.752$, $p = 0.0012$) showing an increase in expression in individuals exposed to STR ($F_{1,46} = 17.04$, $p = 0.0002$) over time and a significant difference between treatments at T_6 ($p = 0.0183$). Expression profiles of *Cabut* for STR and FTR both decreased over time (STR, $F_{1,46} = 6.026$, $p = 0.0179$; FTR, $F_{1,46} = 8.779$, $p = 0.0048$) with time ($F_{7,70} = 3.609$, $p = 0.0022$) and treatment ($F_{7,70} = 7.180$, $p = 0.0231$) explaining a significant amount of variation in gene expression, but only T_2 was significantly different between treatments (Fig. S2, $p = 0.0085$). The serine protease *Stubble* was upregulated in FTR-reared individuals at T_2 ($p = 0.0196$).

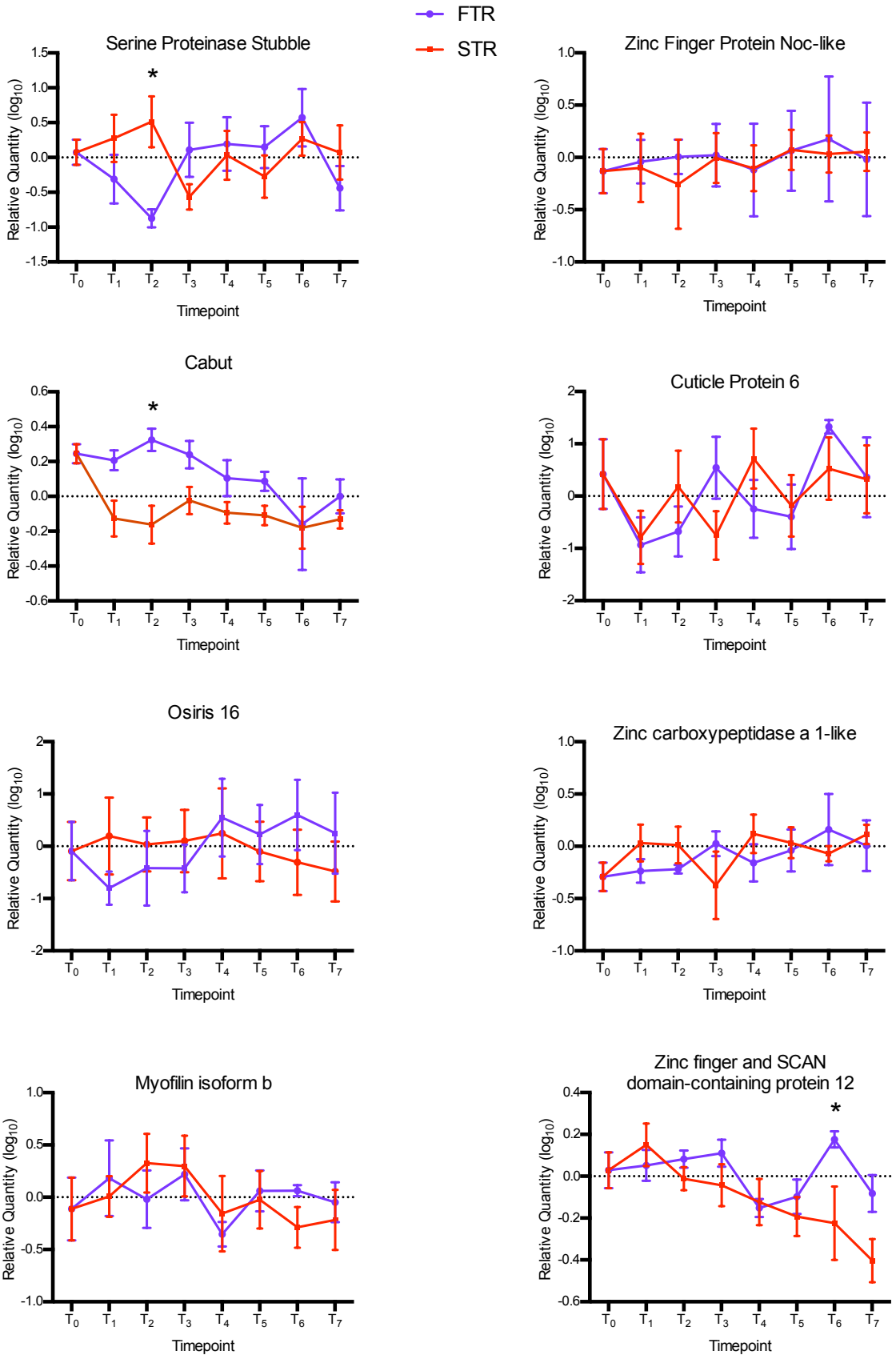

Journal of Experimental Biology • Supplementary information

Figure S1: Biological function gene ontology of differentially expressed transcripts after seven days of low temperature stress.

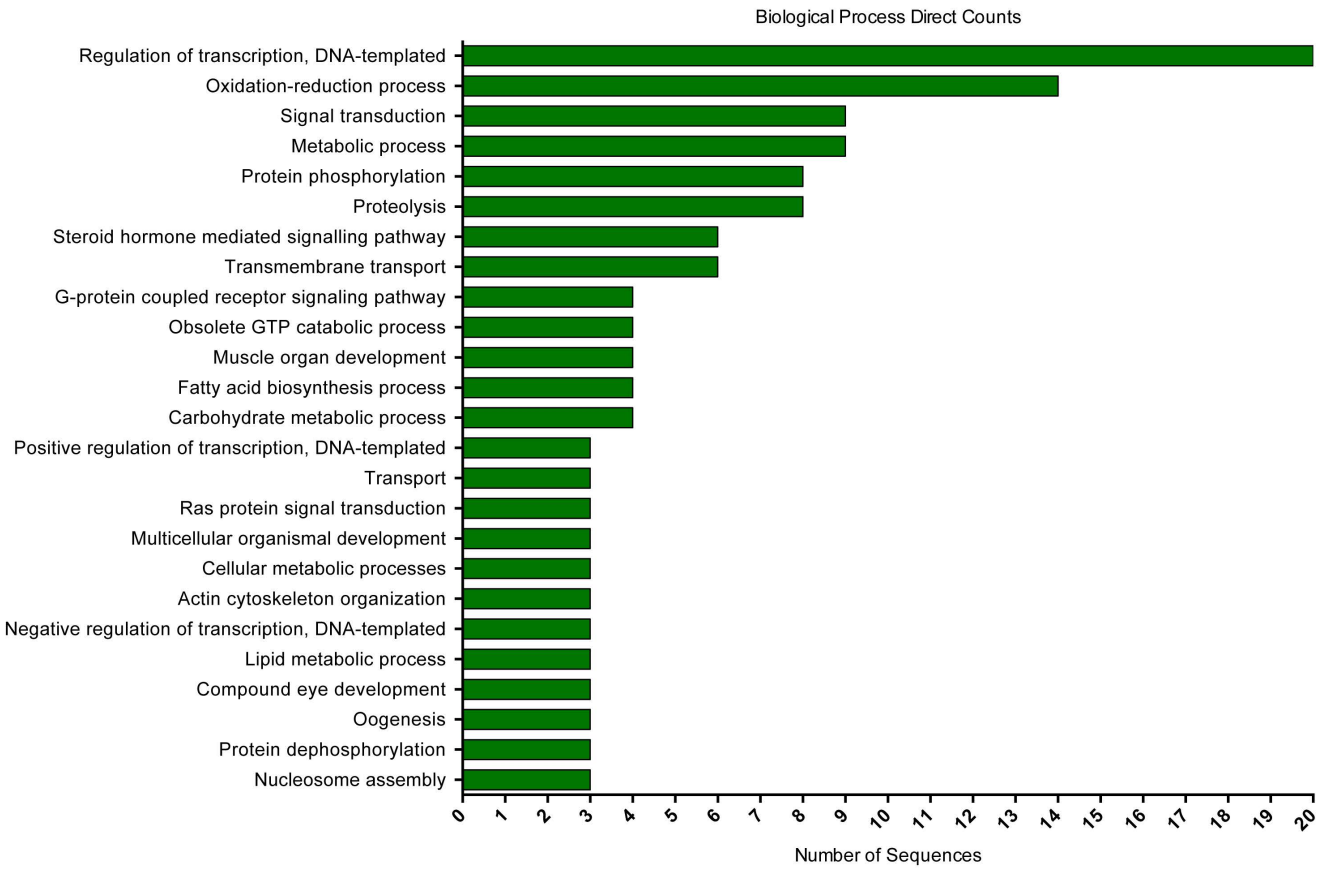

Figure S2: Expression profiles of candidate genes during temperature stress. The expression of candidate genes identified in the RNA-seq analysis was assessed throughout the entire duration of low temperature stress after extended overwintering (n=6). The data are presented as mean ± s.e.m. Asterisks indicate a significant difference in expression between STR and FTR determined by ANOVA.

Table S1. qPCR validation primers. Primer sets highlighted in grey were reference gene candidates.

Transcript ID	Forward	Reverse
MROT_00009775 Set 1	CGA AAC GCT CGC TTA CAA ATA G	CAT TGA GGT GGC TCG TAT CTC
MROT_00009775 Set 2	CCT CAG AGA CAT GAA GGA ACA C	GTG GGA AGA ACT GGG TGA TAT G
MROT_0000590 Set 1	AAT GAG CCT ACG GAA AGA AGA G	GCT TTG GTG CTA GAG GAT GT
MROT_0000590 Set 2	TCG TGC CCT TAC AAA GAC TG	CGA ACT TCT TCT CTC CGG TAT G
MROT_00008799 Set 1	GAC CTG AAC CGA CGT CTT TAA T	CAG TTG ACT CAC AGA GGA GAA C
MROT_00008799 Set 2	CTC CTG GGA ATC AGA TGG TTA G	GGC TTG AAC TCC GCT GAT AA
MROT_00010646 Set 1	GCC GAT ACG ATT GTG AGA GAG	GTT CCA TGT TGG TTC CGT TTC
MROT_00010646 Set 2	ACG CGA GAG GAA CAA CAT AG	GTC GTT GTC CTT CAC CAG AA
MROT_00008869 Set 1	TGC CAA CCA ACA CAA GGA	AGC TAC CGG TTT GCC ATA TT
MROT_00008869 Set 2	CAA AGC CAC AGC ACA CAT TC	ATC GCG ATG ATC TCT GGT TG
MROT_00005226 Set 1	GGC AAA GGG AAT GAC ACT TG	GAG TAC ACA TTC ACA ATC CAT GAG
MROT_00005226 Set 2	CCA ATG GAT GAA TGC CAG AAA T	GAG AAC AAG TGT CAT TCC CTT TG
MROT_00008103 Set 1	GGT CGT GCC AAG ATC AAG AA	CTT AGG CTT CCG AGG ATG ATT G
MROT_00008103 Set 2	CAA TCA TCC TCG GAA GCC TAA G	GCC GAA CAA CCT CTG GAA A
MROT_00002094 Set 1	TGT GAG ATT GGA TGC GAA GAA	CAA CGA GCC TAG CAG AGA TTT A
MROT_00002094 Set 2	GCA TCG GGC AAC AAA TCT TC	CAC GAC TCG TAC GGC TTA AA
MROT_00008639 Set 1	GTG TGG TTA GCA GTT CAG TAG AG	GAA TTT GGC CTT CCT TGT GAT G
MROT_00008639 Set 2	GTT ACG TCC GAG CCT TGA AA	GAG GAA TGC AGC TCA GGA TAA T
MROT_00004919 Set 1	ACA ACC CAC AAC CAG AAG AG	TTC CAC TGT GCA CAT CGT ATT A
MROT_00004919 Set 2	GAG GAG AAT GGC GAT CAC TAA A	CTT CCC TTC GTA GCG TTT CT
MROT_00001385 Set 1	CCA GTT GGT GTT CGA GGA ATA G	TGC TCC AAG TCC AGT GTT ATG
MROT_00002467 Set 1	TAC CTC CTC CTC CGA CTT TAC	CTG GCC GTC CGC ATT ATT A
MROT_00003376 Set 1	CTG GAC CAA AGC AAC AAA CG	CTG GGC CTG TAT CTT CTT CTT C
MROT_00003926 Set 1	GGA GGC GAT CCT ACA AAT ACT G	GTC TAC CTC GAC TTT CTC AAT CG
MROT_0000714 Set 1	CAG TAC ATG CTT TGG CGT TAT G	CCA GAA TCT CCT GTT TCT CCT G
MROT_0000812 Set 1	AGC AGA GAA GAA GAC GAG AAA C	GTG CAG CAG TAC GAC CAA TA
MROT_00008586 Set 1	TGA AAG CTT CTG CGG CTA TTA	CCA ACT TCT GTC TGG TCT CTT C
MROT_00009058 Set 1	GAT GGC AAA CAA GCT AGA AGA AC	GGC TGA TAG AGC AAC GAA CA

Table S2. Ten most up- and down-regulated transcripts after treatment. Log_2 fold change relative to FTR. A negative fold change is an upregulation in STR.

Transcript ID	Sequence Description	Fold Change (log_2)
MROT_00006789	cuticle protein 6	-8.56374
MROT_00008105	osiris 16	-8.42492
MROT_00010933	PREDICTED: uncharacterized protein LOC100879602	-7.38722
MROT_00010985	leucine-rich repeat-containing g-protein coupled receptor 4-like	-6.34828
MROT_00007545	zinc carboxypeptidase a 1-like	-5.2878
MROT_00002812	carboxypeptidase b	-4.91085
MROT_00002813	trypsin-1	-4.91085
MROT_00001862	heavy metal-translocating p-type atpase	-4.42962
MROT_00002788	PREDICTED: hypothetical protein LOC100741758	-4.41335
MROT_00008052	cuticle collagen 3a3	-4.35375
MROT_00009775	tbc1 domain family member 4-like	1.71071
MROT_00005906	cabut	1.72365
MROT_00008799	zinc finger SCAN domain containing protein	1.78574
MROT_00010646	ccaat enhancer-binding protein	1.87841
MROT_00008869	actin-binding rho-activating isoform 1	2.04768
MROT_00005226	seminal fluid protein hacp027	2.07091
MROT_00008103	osiris 14	2.07664
MROT_00002094	zinc finger protein noc-like	2.26969
MROT_00008639	myofilin isoform b	2.33654
MROT_00004919	protein argonaute-2	3.67798

Table S3. qPCR validation. Yellow indicates transcripts that were validated with one primer set and green indicates those validated with two. Genes identified as non-differentially expressed were those used to determine stable reference genes.

Transcript ID	Differentially Expressed in RNA-seq	qPCR Validated
MROT_00009775	Yes	Yes
MROT_00005906	Yes	Yes
MROT_00008799	Yes	Yes
MROT_00010646	Yes	No
MROT_00008869	Yes	Yes
MROT_00005226	Yes	Yes
MROT_00008103	Yes	No
MROT_00002094	Yes	Yes
MROT_00008639	Yes	Yes
MROT_00004919	Yes	Yes
MROT_00001385	No	Yes
MROT_00002467	No	Yes
MROT_00003376	No	Yes
MROT_00003926	No	Yes
MROT_00007147	No	No
MROT_00008127	No	Yes
MROT_00008586	No	Yes
MROT_00009058	No	No

Table S4: Gene ontology of non-cell-membrane transcripts. Log_2 fold change relative to FTR. A negative fold change (grey rows) is an upregulation in STR.

Transcript ID	Function	Transcript	Fold Change
MROT_00000137	Apoptotic Process	death associated protein	-1.04078
MROT_00007022	Apoptotic Process	intraflagellar transport protein 57 homolog	-1.06966
MROT_00004114	Developmental Process	homeobox protein	1.25495
MROT_00005807	Developmental Process	udp-glucose 6-dehydrogenase	1.17127
MROT_00002687	Developmental Process	ras association domain-containing protein 8-like	0.808743
MROT_00006453	Developmental Process	e3 ubiquitin-protein ligase su -like	0.799208
MROT_00010835	Developmental Process	paired box protein pax-2-b	-0.916377
MROT_00000481	Developmental Process	ecdysone-induced protein 78c	-1.30957
MROT_00008639	DNA repair	myofilin isoform b	2.33654
MROT_00004041	DNA repair	dna damage-binding protein 1	1.02919
MROT_00007044	DNA repair	p53 regulated pa26 nuclear protein	0.797203
MROT_00004541	DNA repair	meiotic recombination 11	-1.27712
MROT_00008401	Oxidation-reduction	acyl- delta desaturase-like	-1.17683
MROT_00010957	Oxidation-reduction	acyl- delta desaturase	-1.94342
MROT_00003853	Neurogenesis	isoform b	0.860505
MROT_00004354	Neurogenesis	storkhead-box protein 1	-0.726152
MROT_00002967	Neurogenesis	kn motif and ankyrin repeat domain-containing protein 1	-0.802562
MROT_00007176	Neurogenesis	peptidylglycine alpha-hydroxylating monooxygenase	0.996843
MROT_00007352	Oxidation/reduction	cytochrome b5-related protein	-0.85795
MROT_00000322	Oxidation/reduction	fatty acyl- reductase cg5065-like	-0.954789
MROT_00001392	Oxidation/reduction	probable cytochrome p450 305a1	-1.11015
MROT_00002750	Oxidation/reduction	1-cys peroxiredoxin	-1.35647
MROT_00005092	Oxidation/reduction	d-3-phosphoglycerate dehydrogenase	-1.57624
MROT_00007629	Oxidation/reduction	homogentisate -dioxygenase	-1.57882
MROT_00009098	Oxidation/reduction	pro-phenol oxidase subunit 2	-1.712
MROT_00008416	Oxidation/reduction	cytochrome p450 mitochondrial	-1.73091
MROT_00008044	Oxidation/reduction	oxidase peroxidase	-2.22979
MROT_00009438	Oxidation/reduction	10-formyltetrahydrofolate dehydrogenase	-2.33033
MROT_00003522	Oxidation/reduction	glyoxylate reductase hydroxypyruvate reductase	-2.36061
MROT_00008221	Oxidation/reduction	short-chain dehydrogenase	-2.41981
MROT_00010247	Oxidation/reduction	cytochrome p450 6b1-like	-2.44822

MROT_00000691	Oxidation/reduction	retinol dehydrogenase 14	-2.57532
MROT_00008095	Oxidation/reduction	osiris 2 cg1148-pb	-3.3388
MROT_00000580	Oxidation/reduction	fatty acid synthase	-4.00072
MROT_00000146	Oxidation/reduction	protein kintoun-like	1.41663
MROT_00008499	Oxidation/reduction	cytochrome p450 4g15	-2.2377
MROT_00002050	Stress response	myb domain-containing protein	-2.08356